Published in final edited form as:
J Cell Sci Ther. 2010 October 2; 1(102): . doi:10.4172/2157-7013.1000102.

Non-invasive, Contrast-enhanced Spectral Imaging of Breast Cancer Signatures in Preclinical Animal Models *In vivo*

V Krishnan Ramanujan[1,*] **[Assistant Professor]**, **Songyang Ren**[2] **[Research Scientist I]**, **Sangyong Park**[3] **[Postdoctoral Fellow]**, and **Daniel L Farkas**[4]

[1]Departments of Surgery and Biomedical Sciences, Principal Investigator, Metabolic Photonics Laboratory Cedars-Sinai Medical Center, Los Angeles, CA 90048, USA

[2]Department of Surgery Cedars-Sinai Medical Center, Los Angeles, CA 90048, USA

[3]Department of Surgery Cedars-Sinai Medical Center, Los Angeles, CA 90048, USA

[4]Departments of Surgery and Biomedical Sciences, Cedars-Sinai Medical Center, Los Angeles, CA 90048, USA, Professor, Department of Biomedical Engineering, University of Southern California, Los Angeles, CA, USA

Abstract

We report here a non-invasive multispectral imaging platform for monitoring spectral reflectance and fluorescence images from primary breast carcinoma and metastatic lymph nodes in preclinical rat model in vivo. The system is built around a monochromator light source and an acousto-optic tunable filter (AOTF) for spectral selection. Quantitative analysis of the measured reflectance profiles in the presence of a widely-used lymphazurin dye clearly demonstrates the capability of the proposed imaging platform to detect tumor-associated spectral signatures in the primary tumors as well as metastatic lymphatics. Tumor-associated changes in vascular oxygenation and interstitial fluid pressure are reasoned to be the physiological sources of the measured reflectance profiles. We also discuss the translational potential of our imaging platform in intra-operative clinical setting.

Keywords

Breast cancer; Reflectance; Autofluorescence; AOTF; Spectral imaging

Introduction

Sentinel lymph node (SLN) is the first node in the receiving basin of lymph nodes to which lymphatic drainage from an organ occurs. Axillary staging is an essential prognostic indicator for patients with invasive breast carcinoma [1]. SLN biopsy represents a minimally invasive approach to the surgical management of the axilla for patients with invasive breast cancer. In situations where SLN biopsy is not a viable option, a surgical intervention (lumpectomy and/or radiotherapy) becomes necessary [2,3]. This increases the discomfort and morbidity for patients as well as logistic issues in clinical management of breast cancer.

[*]Corresponding author: V Krishnan Ramanujan, PhD, Assistant Professor, Departments of Surgery and Biomedical Sciences, Principal Investigator, Metabolic Photonics Laboratory Cedars-Sinai Medical Center, Los Angeles, CA 90048, USA, Tel: +1-310-423-7666; Fax: +1-310-423-7707; Ramanujanv@cshs.org.

Our long term goal is to develop and implement high sensitive optical imaging modalities for non-invasive detection of cancer-specific signatures [4]. The rationale behind this goal is that changes in physiological status and the onset of disease pathology such as cancer – would alter the optical properties of mammalian tissues thereby offering a possible avenue for their detection [5-8]. With this motivation, we tested the hypothesis that multispectral reflectance imaging can provide a reliable, non-invasive imaging platform for detecting tumor specific signatures in a preclinical invasive carcinoma in a rat model.

Materials and Methods

Cell culture and tumor generation in rats

Adult female Fisher 344 rats (~180-210 g body weight) were used in these experiments. MAT B-III rat breast cancer cell line was purchased from ATCC and cultured in McCoy's 5a medium supplemented with 10% FCS. In order to generate breast tumor xenografts, the rats were anesthetized by maintaining a steady stream of oxygen/isoflurane by setting up a nose cone/face mask. After removing the hair and sterilizing the skin, 10^6 cells/0.2ml were injected subcutaneously into the mammary fat pads under the rat's nipple. Rats were observed periodically for tumor growth. We observed that the above inoculation protocol generated tumors (100% efficiency) within 2 days and the tumor size reached typically 2-4 cm in 3 weeks. All procedures used were carefully controlled to adhere to the approved institutional animal (IACUC) protocols.

Macroscopic spectral imaging *In vivo*

An Olympus stereo microscope was used for obtaining macroscopic spectral images *ex vivo* and *in vivo*. For exciting the rat breast tissue in live animals, a single-mode optical fiber was attached to a high-power arc lamp source with an in-built monochromator (Polychrome V, TTL photonics). This source offers variable excitation wavelengths (280nm to 694nm) so that the entire spectrum of fluorophores in the visible (and UV) range can be easily excited. On the detection side, we attached a acousto-optic tunable filter (AOTF, Chromodynamics) for collecting reflectance/fluorescence emission from the tissues at specified bandwidths over a broad wavelength range (460nm-1200nm) [9,10]. Spectrally-resolved full-field images were collected by a CCD camera (Orca-ER, Hamamatu Photonics, NJ). Data acquisition and analysis were facilitated by CDI software (QED imaging, Media Cybernetics). Precautions were taken to maintain the body temperature of the rats during the experiments by placing the animal on a heating pad. Rat's limbs were fixed by the adhesive tapes and the body position was very carefully kept under the imaging detector. Respiratory rates were closely monitored by adjusting the concentration of inhaled oxygen/isoflurane mixture, usually at the rate of 30-60/minute. For every excitation wavelength, a complete emission spectral scan was carried out (460nm-750nm; 20nm steps). Typically the first image of the spectral scan constituted the reflectance image and the subsequent images contributed to the fluorescence images. After collecting these spectral images from both the breast and axilla, 50μl of fluorescein (10% w/v in PBS) or 1% lymphazurin was injected subcutaneously into the mammary fat pads or tumors under the nipple using the insulin syringe. The above imaging experimental session was carried out at various time points (5,7,10,14,21 days after cell injection) during the tumor growth. Beyond 21 days, the tumor size became too big and there were signs of ulceration. Therefore we euthanized the rats according to the standard procedures outlined in the institutional IACUC protocol. The tumors, lymph nodes on both sides of the rat were dissected and stored in formalin.

H & E pathology analysis

Standard pathology slides were prepared from representative breast tissues and axillary lymph node tissues and fixed in formalin immediately after harvesting from the rats. Later

these tissues were paraffin fixed and sectioned (5-10 microns) in a microtome for routine H&E staining and visualization.

Immunofluorescence studies

Deparaffinised breast tissues were labeled with primary antibodies (rabbit polyclonal) raised againt key metabolic targets such as Glucose transporter 1 (GLUT1), epidermal growth factor receptor (EGFR), fatty acid synthase (FAS) and Akt. These molecules have been known to be critical in regulating glucose metabolism in breast tumor tissues. Fluorescence visualization of the tissue slides were enhanced by secondary antibodies conjugated with Alexa 488 fluorophore. A wide field fluorescence imaging system was employed in imaging these slides.

Results and Discussion

Figure 1 shows the schematic of the imaging system with the acousto-optic tunable filter. Respiratory rates were closely monitored by adjusting the concentration of inhaled oxygen/ isoflurane mixture, usually at the rate of 30-60 per minute. For every excitation wavelength, a complete emission spectral scan was carried out (460nm-750nm; 20nm steps). Typically the first image of the spectral scan constituted the reflectance image and the subsequent images contributed to the fluorescence images. After collecting these spectral images from both the breast and axilla, 50μl of fluorescein (10% w/v in PBS) or 1% lymphazurin was injected subcutaneously into the mammary fat pads or tumors under the nipple using the insulin syringe. The above imaging experimental session was carried out at various time points (5,7,10,14,21 days after cell injection) during the tumor growth. Beyond 21 days, the tumors became larger (>4 cm) and there were signs of ulceration. Therefore we euthanized the rats according to the standard procedures outlined in the animal protocol. The tumors, lymph nodes from right and left sides of the rat were dissected and stored in formalin. Supporting measurements were carried out from these fixed tissues by standard histopathology and immunofluorescence imaging. All the analyses presented in this study correspond to primary breast tumors and metastatic lymph nodes as confirmed by histopathology. Representative hematoxylin and eosin stained images are shown in Figure 1c.

We first tested if our experimental design could distinguish the primary breast tumors from non-tumor regions as well as from the surrounding autofluorescence and/or vasculature. Figure 2 (a-d) shows spectral reflectance images of the rat breast with 3-week old primary tumor. A spectral emission scan from 480 nm to 694 nm yielded high contrast in visualizing the tumor, vasculature at varying depths without any surgical exposure of the tumors. Although we did not attempt to obtain accurate depths from the top surface of the shaved skin, the obtained images clearly confirmed visualization of tumor vasculature from beneath the rat skin for longer wavelengths (> 600 nm).

A quantitative analysis of the various spectra is shown in Figure 2e where the spectral reflectance and fluorescence signatures of the tumor regions were compared with those of the non-tumor regions (left breast of the same animal in each case). The reflectance signals were significantly lower in tumor regions in the spectral region 460nm-550nm as compared to the non-tumor regions and these observed differences were reproducibly the same in each animal that was studied. Interestingly the autofluorescence signals measured in the tumor region (excitation 480nm; emission ~520nm) were significantly higher in the tumor regions as can be seen in figure 2e as well as figure 2g. No observable autofluorescence signals were present in the spectral regions beyond 560nm. Earlier studies have found that tumor growth also leads to irregular vasculature that is observably different from normal vasculature. In addition to fluorescence visualization of tumor vasculature, it would be valuable to

understand the various components of vascular network *in vivo*. Figure 2e also shows the spectral reflectance profiles of only blood. Low reflectance signals in the spectral region 450-600nm for the blood further confirms that the observed difference between tumor and non-tumor regions arose clearly from the physiological changes in molecular composition in the tumor rather than from the modified vascular network. In fact, a careful comparison of the tumor and non-tumor regions in spectral reflectance profiles in the spectral region beyond 600nm indicate that both these signatures are in good agreement with those of only the blood component. Figure 2h and 2i show the aggressiveness (GLUT1 over expression) and the metastatic potential (circulating tumor cells) of the primary tumor. We then tested if this metastatic potential could be detected by spectral reflectance/fluorescence imaging in the lymph nodes as well. Figure 3 (a-c) show the surgically excised fresh axillary nodes with the surrounding fatty tissue *ex vivo.* Our attempts to inject live MatBIII cells into the surgically excised lymph node tissues (akin to *ex vivo* implantation) did not yield any significant difference in spectral reflectance signatures as can be seen in Figure 3d. One of the major aims of this study was to compare the efficacy of fluorescein in providing better sensitivity to image lymph nodes as compared to the conventionally used absorbance dye lymphazurin. When we injected fluorescein under the nipple as described above and imaged the axillary lymph node non-invasively (without surgical exposure), we found that both the normal and tumor-associated lymphatics had identical fluorescence spectrum for the fluorescein (Figure 3e). However, when the same experiment was carried out after injecting 1% lymphazurin, there was a drastic difference between normal- and tumor-associated lymphatics as can be seen in Figure 3f. This lymphazurin-induced enhanced contrast in spectral reflectance imaging clearly demonstrates an optimal strategy for detecting the physiological changes in the metastatic tumor lymph nodes by the contrast agent such as lymphazurin and a spectrally-resolved imaging platform.

Autofluorescence of the tissue stems mainly from tryptophan, collagen, elastin, NAD(P)H, flavoproteins and porphyrins. The plausible molecular source of the observed difference in spectral reflectance and fluorescence between tumor and non-tumor regions can be flavoproteins (which have emission in the 510-550nm region). Pioneering work by Alfano et al. indicated that ratio of auto fluorescence intensity at 340nm and 440nm could be used to distinguish cancerous and non-cancerous tissues [11]. More recent studies further point out the importance of measuring endogenous tissue fluorescence for disease diagnosis [6,12,13]. A major hurdle in conventional intensity imaging is that skin autofluoresence/reflectance usually obscures the optical signals that emanate from the underlying tumor. This problem stems from the fact that conventional intensity imaging relies on using emission filters (typically 60-80 nm bandwidth) that collect light over a relatively broader range of wavelengths. In our elegant approach of using an AOTF, we overcame this problem by spectral separation of the signals with a narrower (~15-20 nm bandwidth) spectral selection window. Our analysis also revealed that the above spectrally resolved imaging feature adds a reliable method to vascular imaging. As shown in Figure 2e, reflectance profiles around three regions of interest shows significant differences around 460-480nm and 600-640nm windows thereby offering a possibility for ratiometric imaging that could potentially discriminate the skin, blood and tumor vasculature components reliably well. Although fluorescein did not yield any significant advantage over lymphazurin in enhancing spectral reflectance contrast, we did observe that it has advantages in vascular imaging as exemplified in Figure 2f.

Finally, the lymphazurin-induced enhanced contrast in spectral reflectance images of the metastatic lymph node clearly indicates that physiological tissue changes that accompany tumorigenesis/ metastasis can be readily detected non-invasively without surgical complications as confirmed by similar published studies. A plausible explanation for the observed reflectance profiles in the metastatic lymph nodes is that it could arise from local

changes in the vascular oxygenation and/or osmotic pressure around the lymphatics. It is a well-established fact that as the tumor size increases, oxygen partial pressure (pO_2) decreases and the interstitial fluid pressure (IFP) increases [14-16]. It has been hypothesized that these changes could arise from the abnormalities in lymph vessels, leakiness in tumor vasculature as well as due to the contraction of the interstitial space mediated by stromal fibroblasts [16]. As IFP is now considered as a prognostic factor for tumor aggressiveness as well as for the efficacy of chemotherapeutic response in patients with advanced tumors, Figure 3f points to an interesting possibility for non-invasive monitoring of the changes in the metastatic lymph nodes thereby augmenting the current approaches for staging the tumors and monitoring chemotherapy response.

Conclusions and Future Perspectives

In conclusion, we have demonstrated a viable, imaging platform for real-time monitoring of tumors in preclinical rat models of breast cancer where tumor-specific spectral signatures could be imaged non-invasively with an AOTF. Early detection of tumors is the key to effective therapeutic intervention and successful patient survival. Our results demonstrate an attractive strategy that can augment the existing clinical imaging repertoire with added advantages of higher spatial resolution and non-ionizing radiation. Since the contrast agents (lymphazurin and fluorescein) employed in this study are already in clinical use, the next logical step would be to extend these studies in a clinical setting with appropriate imaging system adaptations. AOTF, owing to its high speed acquisition, can provide a useful multimodality platform in conjunction with fast fluorescence lifetime imaging system thereby increasing sensitivity and accuracy in tumor imaging applications [17,18].

Acknowledgments

We gratefully acknowledge financial support from Susan G Komen for Cure foundation (Career Catalyst Research Award #KG090239), National Cancer Institute/National Institutes of Health (ARRA Stimulus Award #R21-CA124843), and institutional support from the Department of Surgery (all to V.K.R.), the US Navy Bureau of Medicine and Surgery (Award # 1435-04-04- CA-43096) and National Science Foundation (BESOO 79483) (both to D.L.F.).

References

1. Rovera F, Frattini F, Marelli M, Corben AD, Dionigi G, et al. Axillary sentinel lymph node biopsy: an overview. Int J Surg. 2008; 6:S109–112. [PubMed: 19131285]
2. Keshtgar M, Hamidian JA, Davidson T, Escobar P, Mallucci P, et al. Tissue screening after breast reduction. BMJ. 2009; 338:b630. [PubMed: 19278972]
3. Keshtgar MR, Chicken DW, Tobias JS. New approaches in breast cancer management: sentinel node biopsy and intraoperative radiotherapy. Int J Fertil Womens Med. 2005; 50:218–226. [PubMed: 16468472]
4. Nyirenda N, Farkas DL, Ramanujan VK. Preclinical evaluation of nuclear morphometry and tissue topology for breast carcinoma detection and margin assessment. Breast Cancer Res Treat. 2010 Epub ahead of print.
5. Esposito A, Schlachter S, Schierle GS, Elder AD, Diaspro A, et al. Quantitative fluorescence microscopy techniques. Methods Molecular Biol. 2009; 586:117–142.
6. Ramanujan VK, Zhang JH, Biener E, Herman B. Multiphoton fluorescence lifetime contrast in deep tissue imaging: prospects in redox imaging and disease diagnosis. J Biomed Opt. 2005; 10:051407. [PubMed: 16292944]
7. Shehada RE, Marmarelis VZ, Mansour HN, Grundfest WS. Laser induced fluorescence attenuation spectroscopy: detection of hypoxia. IEEE Trans Biomed Eng. 2000; 47:301–312. [PubMed: 10743771]

8. Svanberg K, af Klinteberg C, Nilsson A, Wang I, Andersson-Engels S, et al. Laser-based spectroscopic methods in tissue characterization. Ann NY Acad Sci. 1998; 838:123–129. [PubMed: 9511801]
9. Shonat RD, Wachman ES, Niu W, Koretsky AP, Farkas DL. Near-simultaneous hemoglobin saturation and oxygen tension maps in mouse brain using an AOTF microscope. Biophys J. 1997; 73:1223–1231. [PubMed: 9284290]
10. Wachman ES, Niu W, Farkas DL. AOTF microscope for imaging with increased speed and spectral versatility. Biophys J. 1997; 73:1215–1222. [PubMed: 9284289]
11. Alfano RR, Das BB, Cleary J, Prudente R, Celmer EJ. Light sheds light on cancer--distinguishing malignant tumors from benign tissues and tumors. Bull NY Acad Med. 1991; 67:143–150.
12. Andersson-Engels S, Klinteberg C, Svanberg K, Svanberg S. In vivo fluorescence imaging for tissue diagnostics. Phys Med Biol. 1997; 42:815–824. [PubMed: 9172261]
13. Keller MD, Majumder SK, Kelley MC, Meszoely IM, Boulos FI, et al. **A**utofluorescence and diffuse reflectance spectroscopy and spectral imaging for breast surgical margin analysis. Lasers Surg Med. 2010; 42:15–23. [PubMed: 20077490]
14. Brown JQ, Wilke LG, Geradts J, Kennedy SA, Palmer GM, et al. Quantitative optical spectroscopy: a robust tool for direct measurement of breast cancer vascular oxygenation and total hemoglobin content in vivo. Cancer Res. 2009; 69:2919–2926. [PubMed: 19293184]
15. Bird B, Bedrossian K, Laver N, Miljkovic M, Romeo MJ, et al. Detection of breast micro-metastases in axillary lymph nodes by infrared micro-spectral imaging. Analyst. 2009; 134:1067–1076. [PubMed: 19475131]
16. Heldin CH, Rubin K, Pietras K, Ostman A. High interstitial fluid pressure – an obstacle in cancer therapy. Nat Rev Cancer. 2004; 4:806–813. [PubMed: 15510161]
17. Jo JA, Fang Q, Marcu L. Ultrafast Method for the Analysis of Fluorescence Lifetime Imaging Microscopy Data Based on the Laguerre Expansion Technique. IEEE J Quantum electron. 2005; 11:835–845. [PubMed: 19444338]
18. Shrestha S, Applegate BE, Park J, Xiao X, Pande P, et al. High-speed multispectral fluorescence lifetime imaging implementation for in vivo applications. Opt lett. 2010; 35:2558–2560. [PubMed: 20680057]

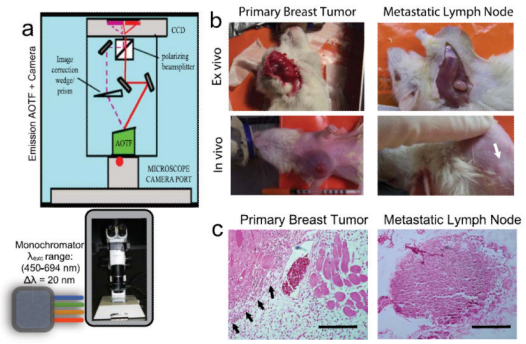

Figure 1.

(a) Schematic of the multispectral imaging system involving a strategic assembly of the stereo microscope (Olympus SZX12), a multi-wavelength excitation light source with a monochromator (Polychrome, TTL), the emission acousto-optic tunable filter (Chromodynamics Inc, FL, USA) and a CCD camera (Orca ER, Hamamatsu photonics, USA). Data acquisition and analysis were performed using CDI *Invivo* software (Media Cybernetics, MD, USA). (b) Representative photographs of the anesthetized rats ~10 days after the tumor generation. Tumor xenografts were generated in the right breast of the animal so that the left breast served as a non-tumor control in each animal studied. *Ex vivo* images were obtained by excising the shaved skin and exposing the primary tumor or the metastatic lymph node as shown in the top panel. The white arrow indicates the location of the lymph node around which the *in vivo* images were obtained. (c) Representative histopathology slides (H&E staining) of the tissue slices obtained from the primary breast tumor tissue and the metastatic lymph node tissue. Scale bars = 50μm. The black arrows indicate the margin between the tumor and normal tissue regions.

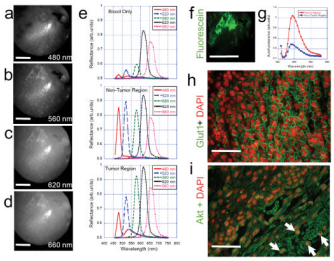

Figure 2. Primary Breast Tumor

(a) – (d) Representative In vivo spectral reflectance images of the primary breast tumor 10 days after injection. On day 10, the rats were anesthetized and 10% fluorescein and/or 1% lymphazurin was injected right under the breast nipple. After 15 minutes of dye equilibration, tumors were excited with light from the Polychrome light source (450nm-694nm in consecutive bandwidths of 20nm) and multispectral AOTF images were obtained for each excitation band (460nm-750nm range; $\Delta\lambda$= 20nm). For every excitation, the first image in the emission window constituted the reflectance image while the rest of the images in the series constituted the fluorescence images. Reflectance images at longer wavelengths (> 560 nm) clearly show tumor vasculature details below the shaved skin of the animal. (e) Graphical display of reflectance spectra in normal (left) and tumor (right) breasts from an animal after 10- days of tumor growth. The reflectance spectral signatures for 480, 520 and 580 nm excitation are significantly different between the tumor and normal breasts thereby indicating possibilities for quantitative imaging of tumor-specific signatures in tumor xenografts without surgical incision. The figure also shows the spectral reflectance profiles for blood from the same animal. (f) fluorescence image of tumor vasculature after fluorescein injection in the tumor breast (Scale bar = 1cm) and (g) auto fluorescence spectra from tumor and non-tumor breasts (h) representative immunofluorescence image obtained from a section of the breast tumor tissue showing upregulation of the glucose transporters (GLUT-1) that is a measure of tumor aggressiveness in vivo as well as (i) the metastastic potency of these tumor cells (indicated by white arrows) as shown by Akt-Alexa488 immunofluorescence labeling of the blood vessel where tumor cells are found amidst anucleated red blood cells. Scale bars = 20μm.

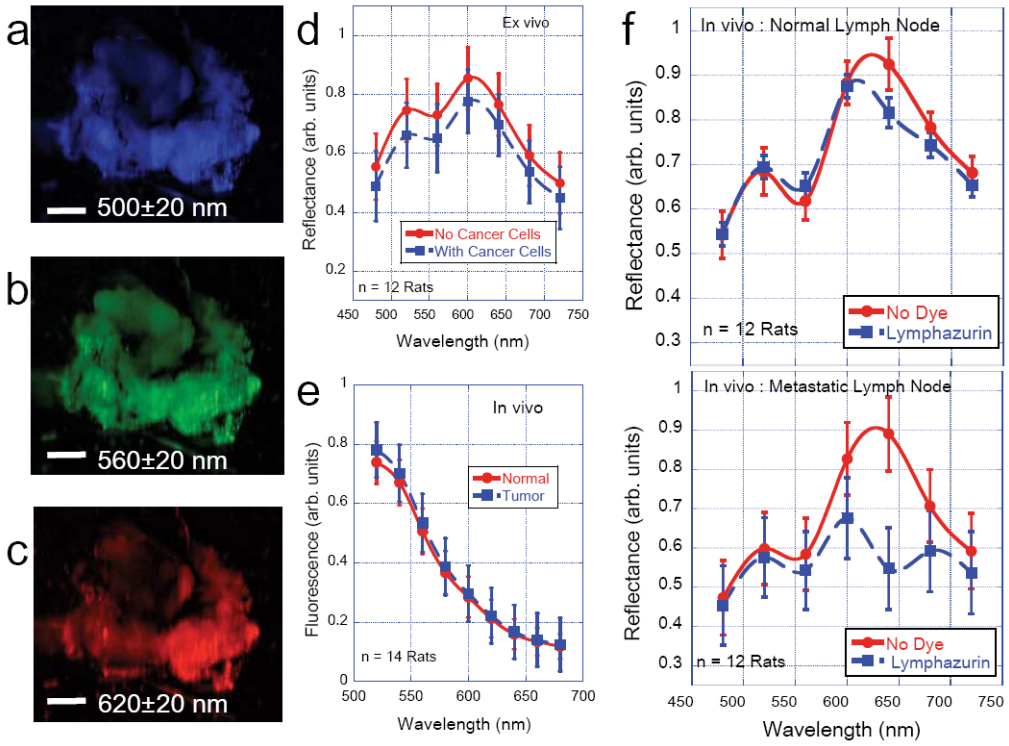

Figure 3. Metastatic Lymph Node

(a)-(c) Representative spectral reflectance images of the lymph node along with the surrounding fatty tissues isolated from rat model. Scale bars = 1mm. As can be seen from the images and from the accompanying graph (d), the reflectance signal has maxima at 500nm and 620 nm. The plot shown is an average of reflectance profiles from 12 animals (Mean ± *SEM*). The figure (d) also shows that there is no significant difference in the observed spectral reflectance profile even when live cells (1×106 cancer cells) were injected into the lymph node tissues *ex vivo*. (e) Average In vivo fluorescence profiles (n= 14 rats) obtained after injecting 10% fluorescein dye under the nipple. The comparison of fluorescein profile between normal and tumor-associated lymphatics showed no observable difference. However, when 1% lymphazurin dye was injected under the nipple instead of fluorescein, there was an observable difference in spectral reflectance profiles in the normal lymph nodes *in vivo* (f) See main text for more details.